

Franz–Keldysh Effect in GaN Nanowires

A. Cavallini, L. Polenta,* and M. Rossi

*Physics Department and CNISM, University of Bologna, Viale Berti Pichat 6/2,
40127 Bologna, Italy*

T. Stoica, R. Calarco, R. J. Meijers, T. Richter, and H. Lüth

*Institute of Bio- and Nanosystems (IBN1) and CNI—Center of Nanoelectronic Systems
for Information Technology, Research Centre Jülich, 52425 Jülich, Germany*

Received April 23, 2007; Revised Manuscript Received May 21, 2007

ABSTRACT

Surface photovoltage spectroscopy and spectral photoconductivity measurements have been carried out in the UV spectral region on GaN nanowires to analyze the near band-edge region. The results reveal the presence of tails in the band–band absorption spectra. Surface Photovoltage spectra performed on the as-grown nanowire ensemble show a long band tail of about 0.1 eV. Spectral photoconductivity on singly contacted nanowires shows that the band tail width strictly depends on the wire diameter. These results are explained by the Franz–Keldysh effect due to the internal electric field induced by Fermi level pinning at the nanowire surface. The experimental values of the absorption tail are well in agreement with the results obtained by simulating the electric field in a cylindrical model.

In recent years, nitride-based nanostructures have been attracting high interest in view of their electronic and optoelectronic applications.^{1–7} In particular, GaN nanowires (NWs)^{6–10} are considered as prospective materials for the fabrication of future optoelectronic, high-power, and high-operation temperature devices. To address this challenge, however, a deep knowledge of the influence of nanoscale size on their electrical and optoelectronic properties is required.

An important issue, addressed in the present paper, concerns the study of optoelectronic properties of GaN-NWs in the band-edge region. Because the standard methods for absorption measurements are hardly applicable on nanostructures due to technical and geometrical constraints, alternative characterization techniques are required to explore the band-edge features. Surface photovoltage spectroscopy (SPS)¹¹ and spectral photoconductivity (SPC)¹² techniques have been applied to characterize the near band-edge absorption in GaN-NWs.

GaN-NWs here analyzed were grown on Si (111) substrates by plasma-assisted molecular beam epitaxy (MBE). A detailed description of the growth procedure is elsewhere reported.⁶ The as-grown sample showed a wide distribution of hexagonal wires with diameters ranging from 20 to 500 nm and lengths from 0.3 up to 2 μm .

Because SPS¹¹ is a noncontact technique, noninvasive and nondestructive, it results in a very suitable method for characterizing samples containing the as-deposited nanowires ensemble (an SEM picture of this type of sample is shown

in the inset of Figure 1a). Absorption spectra have been obtained at room temperature using a xenon lamp and a SPEX 500M monochromator as a monochromatic light source. The sample was capacitively coupled to a metallic semitransparent electrode, which is the SPS probe. The voltage signal was measured by a unit gain FET pre-amplifier (used as current–voltage converter) and then collected by a lock-in amplifier (Stanford Research Systems model SR830DSP). SPS measurements were performed on the large ensemble of nanowires under the SPS electrode area (about 3–4 mm²).

Figure 1a shows the typical SPS spectrum obtained in the band-edge region of NWs. The SPS signal V_s significantly increases when the optical excitation energy varies from 3.3 to 3.5 eV in the band-edge absorption region. This behavior is characteristic of a band-to-band transition of an n-type semiconductor. The increase of V_s corresponds to the minority carrier (holes) accumulation caused by the optical generation of electron–hole pairs near to the surface: the electrons move toward the bulk due to the electric field in the surface space charge region, while holes are collected at the surface barrier.

For a direct band gap material such as GaN, the following relationship holds,^{13–15}

$$h\nu \times V_s \propto (h\nu - E_{\text{gap}})^{1/2} \quad (1)$$

where E_{gap} is the energy gap and $h\nu$ the photon energy of the optical excitation.

The energy gap E_{gap} , evaluated from the intercept of the linear fitting of $(V_s \times h\nu)^2$ as a function of $h\nu$ (Figure 1b),¹⁶

* Corresponding author. E-mail: laura.polenta@unibo.it.

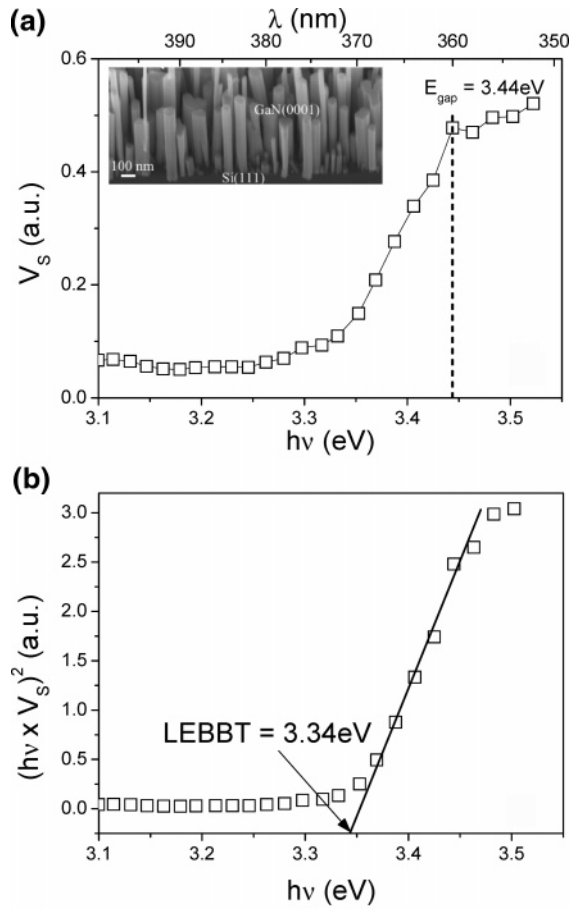


Figure 1. (a) Typical SPS spectrum where E_{gap} is estimated by the knee (in the inset a SEM picture of ensemble NW sample is shown); (b) the fitting curve of the linear region $(h\nu \times V_s)^2$ vs $h\nu$ is shown and LEBBT value is calculated as x -intercept.

results in 3.34 ± 0.03 eV, significantly lower than the bulk band gap energy reported in literature.¹⁷ From the spectrum, it is however evident that the transition is affected by a large band tail, reasonably due to the significant contribution of sub-band gap absorption, dramatically affecting the slope of the diagram in Figure 1b and, in turn, the intercept of the linear fit.^{18,19} Thus it is reasonable to estimate the energy gap by the energy corresponding to the knee in the SPS spectrum of Figure 1a, i.e., $E_{\text{gap}} = (3.44 \pm 0.05)$ eV, and to consider the value (3.34 ± 0.03) eV as the lowest energy band-to-band transition (LEBBT) due to the band tails. The difference $\Delta E_{\text{SPS}} = 0.10$ eV between E_{gap} and LEBBT is therefore the band tail width averaged on whiskers with different diameters.

To investigate a possible dependence of ΔE_{SPS} from nanowire width, SPS would have to be carried on singly contacted nanowires of different thickness, but in this case, the macroscopic SPS electrode cannot be capacitively coupled to a single nanowire. Spectral photoconductivity (SPC) was therefore carried out on over 20 isolated nanowires, with diameters ranging between 40 and 500 nm with ohmic contacts (an SEM picture of the device is shown in the inset of Figure 2a). The procedure for the fabrication of single nanowire devices is described elsewhere, where also the I - V characteristics are reported showing the ohmic behavior of

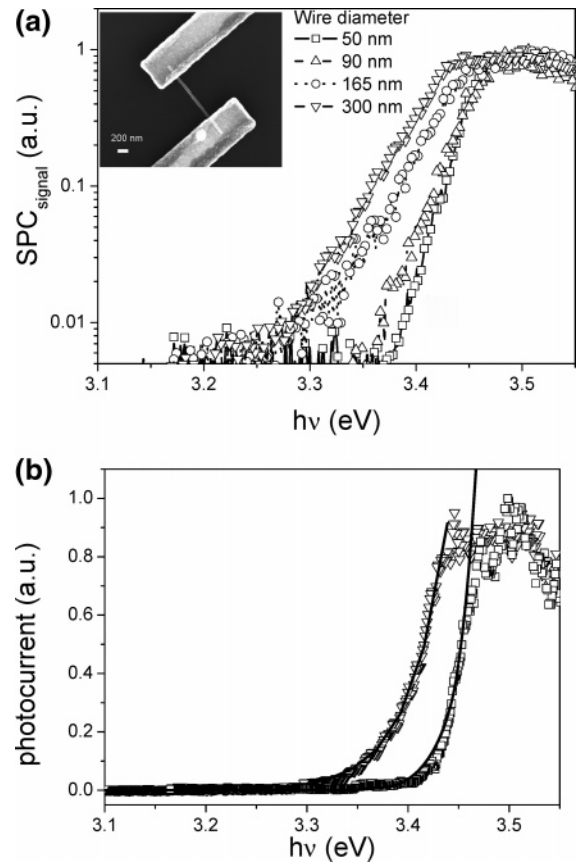


Figure 2. (a) Typical SPC spectra obtained on nanowires of different diameters: \square 50 nm, \triangle 90 nm, \circ 165 nm, and ∇ 300 nm (in the inset a SEM picture of single NW is shown); (b) exponential fit of SPC spectra obtained on \square 50 nm and ∇ 300 nm diameter wires.

contacts.⁷ Therefore, we can state that the internal electric field can only be ascribed to the depletion region at the nanowire surface and not to a possible space charge region at the contacts, as previously investigated by Gu and co-workers.²⁰

For spectral photoconductivity measurements, a dc voltage is supplied in order to keep a constant electric field driving the carriers through the electrodes and maintaining similar conditions of operation for all measurements. The photocurrent signal has been collected by a lock-in amplifier and subsequently normalized to the photon flux. Measuring the current value due to the release of carriers toward the bands the energy value for intrinsic and extrinsic absorptions can be evaluated.²¹

Typical SPC spectra measured on single NW devices with different diameter are reported in Figure 2a, showing similar band tails as in SPS measurements. The sub-band-edge contribution clearly increases with nanowire diameter. For a better comparison, two photoconductivity spectra for the thinnest and thickest diameter have been represented in linear scale in Figure 2b. The photoconductivity variation $\Delta\sigma$ is expressed by the equation:

$$\Delta\sigma = e\beta\alpha\Phi(1 - R)(1 - e^{-\alpha x})(\mu_n\tau_n + \mu_p\tau_p) \quad (2)$$

where e is the electron charge, β the carrier pairs generated

by each photon, α is the absorption coefficient, Φ the photon flux, R the reflection coefficient, x the penetration depth, and μ and τ the mobility and lifetimes of both carriers, respectively. For nanowires, whose diameter ranges in the order of hundreds of nanometers, the term $(1 - e^{-\alpha x})$ can be reasonably considered constant in the band-edge region, hence photoconductivity results proportional to the absorption coefficient α . The SPC absorption tails of Figure 2b have been therefore well fitted by the exponential law:

$$PC \sim \alpha \sim \exp(h\nu/\Delta E_{\text{SPC}}) \quad (3)$$

Generally speaking, an absorption tail close to the band-to-band transition can be ascribed to different phenomena, as for example structural disorder, defects or impurities, doping fluctuations, as well as broad excitonic, phononic, or plasmonic absorption or the presence of a strong electric field (Franz–Keldysh effect).²² This last hypothesis results as the most plausible for the observed effects in band tails. In GaN nanowires, a strong electric field exists in a depletion region due to the Fermi level pinning on the wire surface as demonstrated in ref 7. This surface depletion region of a high electric field can have an essential contribution in sub-band photoeffects due to Franz–Keldysh effect, especially for the case of NWs with a high surface–volume ratio than for compact layers. Results of high-resolution TEM investigation shown a nearly perfect crystalline structure,²³ which is not compatible with an absorption tail due to structural disorder. As a matter of fact, if structural disorder is considered responsible for the diameter dependence of the of the band tails, we should accept that the disorder increases substantially with the wire diameter. To achieve values of about 40 meV for the specific energy of the absorption band tail, as observed in our measurements, we should assume a high disorder like in amorphous materials.²⁴ Moreover, electrical-photoelectrical measurements on single NW devices demonstrated a relative low carrier concentration ($6.25 \times 10^{17} \text{ cm}^{-3}$),⁷ allowing for excluding mechanisms other than the Franz–Keldysh effect. Excitonic effects or Coulomb interaction is included in Franz–Keldysh effect, as discussed later in this paper. The other aforementioned band-edge absorption effects, if present, are expected to be masked as the excitonic effect in GaN at room temperature is the dominating one.²²

The Franz–Keldysh effect is a physical phenomenon associated to the influence of a high electric field on the near band-edge absorption.²² Franz²⁵ and Keldysh²⁶ predicted that the electric field may cause a red-shift of the absorption edge, giving rise to the presence of an absorption tail for band-to-band transitions. In 1966, Duke²⁷ modeled the optical-absorption coefficient tail, and in 1970, Dow et al.²⁸ accounted for the alteration of the Franz–Keldysh absorption edge induced by electron–hole scattering (excitonic contribution) with electric field strengths on the order of 10^5 V/cm .

In GaN nanowires, due to the Fermi level pinning at the wire surface, a strong electric field exists in the depletion region,⁷ which plays a fundamental role in sub-band photoeffects, especially for the case of NWs with a high surface–volume ratio with respect to that of compact layers.

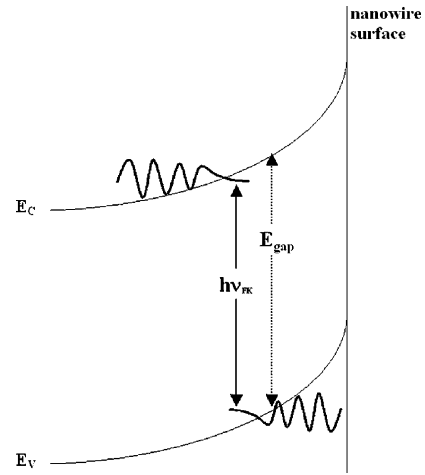


Figure 3. Sketch of the band structure of a n-type semiconductor surface: the wave function of an electron in the conduction band and a hole in the valence band are characterized by tails in the forbidden band gap induced by the internal electric field (Franz–Keldysh effect): the band to band transition occurs at an energy $h\nu$ lower than the energy gap.

Under a constant electric field, the free electron wave function modifies into an Airy function, which exponentially decreases in the band gap region. As a result, a sub-band gap optical absorption occurs, which can be interpreted as a photon-assisted tunneling through the forbidden band region, with photon energy smaller than E_{gap} (Figure 3).

In the sub-band region, the Franz–Keldysh absorption coefficient vs $h\nu$ can be approximated by an exponential function:^{29,30}

$$\alpha(h\nu) \sim \exp\left(-\left|\frac{h\nu - E_{\text{gap}}}{\Delta E}\right|^{3/2}\right) \quad (4)$$

with ΔE given by:¹²

$$\Delta E = \frac{2}{3} \frac{(e\hbar\xi)^{2/3}}{(m^*)^{1/3}} \quad (5)$$

where ξ , m^* , e , and \hbar are the electric field, effective mass, electron charge, and Planck constant ($\hbar/2\pi$), respectively.

As theoretically predicted,²⁸ deviation from the classical shape (eq 4) of the Franz–Keldysh absorption tail might be explained by taking into account the excitonic interaction, which in GaN has been detected even at room temperature.³¹ The computed curves based on the influence of the excitonic interaction on the Franz–Keldysh effect are characterized by a simple exponential tail for a large range of the model parameters²⁸ and correspond to the fitting of our SPC absorption tails (eq 3).

To check the validity of our hypotheses, we simulated the band tail widths ΔE following eq 5 by modeling the electric field distribution $\xi(r)$ in NWs. This cylindrical model already proposed to explain the strong diameter dependence of the NW conductivity in the dark as well as under UV light was used.⁷ Because of Fermi level pinning at the GaN NW

surface, band bending appears in the surface depletion region: a critical diameter d_{crit} for completely depleted wires has been defined, i.e., wires with lateral dimensions lower than d_{crit} result in being completely depleted. Larger wires may contain a tight core conductive channel. A uniform distribution of donors inside the wire was assumed. In this case, the electric field $\xi(r)$ and the potential $V(r)$ inside of thinner wires with $d < d_{\text{crit}}$ is given by:

$$\xi(r) = \frac{eN_d}{2\epsilon} r \quad (6)$$

$$V(r) = -\frac{eN_d}{4\epsilon} r^2 \quad (7)$$

where r is the wire radius, N_d the donor concentration, and ϵ the electrical permittivity.

In wires with $d > d_{\text{crit}}$, a surface depletion region of width W and a core region with radius $r < d/2 - W$, where $\xi(r) \approx 0$ and $V(r) \approx 0$ take place. In the space charge region for $r > d/2 - W$, we have:

$$\xi(r) = \frac{eN_d}{2\epsilon} \left(r - \frac{(d/2 - W)^2}{r} \right) \quad (8)$$

$$V(r) = -\frac{eN_d}{4\epsilon} \left(r^2 - (d/2 - W)^2 \left(1 + 2 \ln \frac{r}{(d/2 - W)} \right) \right) \quad (9)$$

The electric field and the band bending achieve their maximum values ξ_0 and $-eV_0$ at the surface, i.e., $\xi_0 = \xi(d/2)$ and $-eV_0 = -eV(d/2)$. For wires with $d > d_{\text{crit}}$, the surface band bending barrier ϕ is equal to the Fermi level pinning energy ϕ_0 relative to the unperturbed conduction band, while for $d < d_{\text{crit}}$, it decreases with the wire diameter. According to this model, a critical diameter ~ 80 nm and a Fermi level pinning energy $\phi_0 = 0.55$ eV were extracted as fitting parameters in ref 7 in agreement with other theoretical and experimental studies.^{32–34}

In Figure 4a, the calculated diameter dependence of the surface electric field ξ_0 is shown. A strong diameter dependence of the electric field values is obtained for $d < d_{\text{crit}}$.

The ξ_0 keeps increasing for $d > d_{\text{crit}}$ due to the diameter dependence of the depletion width $W(d)$. The electric field in the depletion region and its associated Franz–Keldysh effect can explain the diameter dependence of the absorption tail as experimentally observed in the SPC curves (Figure 2). By the surface electric field ξ_0 and eq 5, the tail energy as a function of the wire diameter can be estimated. The experimental values of the exponential tail energy ΔE_{SPC} show a good agreement with the calculated trend, as reported in Figure 4b.

To explain the absorption tail observed in SPS measurements, we have to keep in mind that these measurements are performed on samples with a large ensemble of NWs. As a consequence, the spectral tail is strongly influenced by the wire statistics. Besides fluctuations of the surface electric field due to diameter variations, additional fluctuations due to different doping and structural defects in shorter and longer

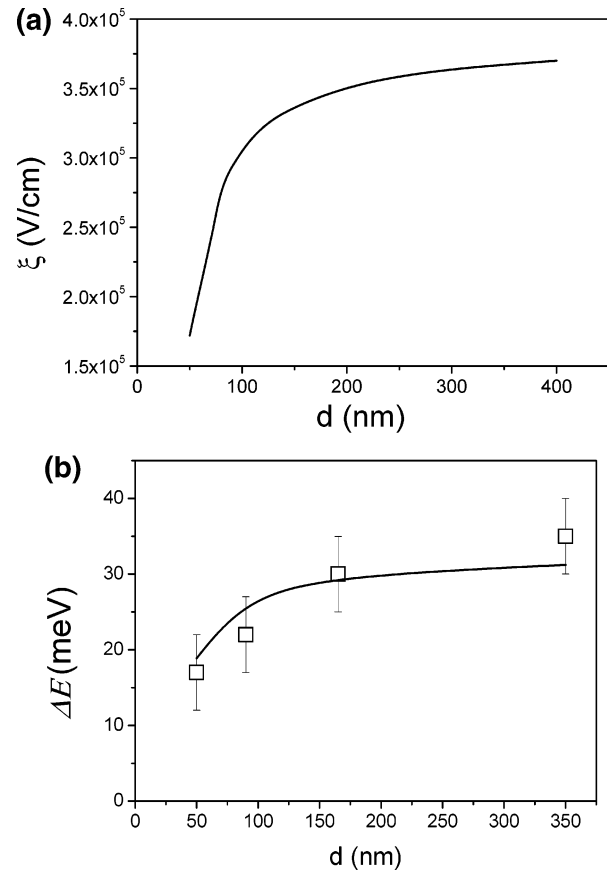


Figure 4. (a) Calculated electric field as a function of nanowire diameter; (b) comparison between the simulated curve of Franz–Keldysh tail and band tail data obtained from PC spectra.

wires are present. If we compare the SPS curve in Figure 1a with the curve of the thicker wire in Figure 2, we can see that the tail width has approximately the same value. We can therefore conclude that the SPS tail signal is dominated by the contribution of thicker and shorter wires, which is the majority of the wires present in the sample.

In conclusion, the spectral band-edge absorption of GaN NWs, studied by SPS and SPC, shows an exponential tail below the energy gap. A strong dependence of the band absorption tail as a function of wire diameter was found by SPC measurements performed on single wires. The band-edge tailoring and its wire-diameter dependence can be explained by the Franz–Keldysh effect induced by the electric field in the depletion region of the wire surface. The tail of the band-edge absorption observed in SPS curves is an average value reflecting the distribution of differently sized nanowires in the as prepared sample. The experimental absorption tails fit well to a single-exponential function $\exp(h\nu/\Delta E)$, suggesting a strong influence of the Coulomb (exciton) interaction on the Franz–Keldysh effect. The electric field dependence of the band tail energy ΔE has been calculated using a cylindrical model for the estimation of the electric field in the depletion region of the nanowire surface. Good agreement was obtained between theoretical simulation of the Franz–Keldysh absorption tail and experimental data obtained by SPS and SPC measurements.

Acknowledgment. We thank K. H. Deussen for technical support and M. Marso for processing of single NW devices. This research was carried out in the framework of the VIGONI program (www.crui.it) funded by Ministero Istruzione Università e Ricerca (MIUR) and Deutscher Akademischer Austauschdienst (DAAD).

References

- (1) Greytak, A.; Lauhon, L.; Gudiksen, M.; Lieber, C. *Appl. Phys. Lett.* **2004**, *84*, 4176.
- (2) Duan, X.; Huang, Y.; Agarwal, R.; Lieber, C. *Nature* **2003**, *421*, 241.
- (3) Zhong, Z.; Wang, D.; Cui, Y.; Bockrath, M.; Lieber, C. *Science* **2003**, *302*, 1377.
- (4) Bjork, M.; Ohlsson, B.; Thelander, C.; Persson, A.; Deppert, K.; Wallenberg, L.; Samuelson, L. *Appl. Phys. Lett.* **2002**, *81*, 4458.
- (5) Bjork, M.; Ohlsson, B.; Sass, T.; Persson, A.; Thelander, C.; Magnusson, M.; Deppert, K.; Wallenberg, L.; Samuelson, L. *Appl. Phys. Lett.* **2002**, *80*, 1058.
- (6) Meijers, R.; Richter, T.; Calarco, R.; Stoica, T.; Bochem, H.-P.; Marso, M.; Lüth, H. *J. Cryst. Growth* **2006**, *289*, 381.
- (7) Calarco, R.; Marso, M.; Richter, T.; Aykanat, A. I.; Meijers, R.; v. d. Hart, A.; Stoica, T.; Lüth, H. *Nano Lett.* **2005**, *5*, 981.
- (8) Sánchez-Páramo, J.; Calleja, J.; Sánchez-García, M.; Calleja, E.; Jahn, U. *Physica E* **2002**, *13*, 1070.
- (9) Calleja, E.; Sánchez-García, M.; Sánchez, F.; Calle, F.; Naranjo, F.; Muñoz, E.; Jahn, U.; Ploog, K. *Phys. Rev. B* **2000**, *62*, 16826.
- (10) Ristic, J.; Calleja, E.; Sánchez-García, M.; Ulloa, J.; Sánchez-Páramo, J.; Calleja, J.; Jahn, U.; Trampert, A.; Ploog, K. *Phys. Rev. B* **2003**, *68*, 125305.
- (11) Kronik, L.; Shapira, Y. *Surf. Interface Anal.* **2001**, *31*, 954–965.
- (12) Bube, R. H. *Photoconductivity of Solids*; Wiley: New York, 1960.
- (13) Adamowicz, B.; Szuber, J. *Surf. Sci.* **1991**, *247*, 94.
- (14) Litovchenko, V. G.; Popov, V. G. *Sov. Phys. Semicond.* **1982**, *16*, 472.
- (15) Kalnitsky, A.; Zukotynski, S.; Sumski, S. *J. Appl. Phys.* **1981**, *52*, 4744.
- (16) Kronik, L.; Shapira, Y. *Surf. Sci. Rep.* **2001**, *31*, 954–1265.
- (17) Edgar, J. H. *Properties of Group III Nitrides*; INSPEC, The Institution of Electrical Engineers: London, 1994.
- (18) Gal, D.; Mastai, Y.; Hodes, G.; Kronik, L. *J. Appl. Phys.* **1999**, *86*, 5573.
- (19) Ambacher, O.; Rieger, W.; Ansmann, P.; Angerer, T. H.; Moustakas, D.; Stutzman, M. *Solid State Commun.* **1996**, *97*, 365–370.
- (20) Gu, Y.; Kwak, E. S.; Lensch, J. L.; Allen, J. E.; Odom, T. W.; Lauhon, L. J. *Appl. Phys. Lett.* **2005**, *87*, 043111.
- (21) Cavallini, A.; Polenta, L.; Rossi, M.; Richter, T.; Marso, M.; Meijers, R.; Calarco, R.; Luth, H. *Nano Lett.* **2006**, *6*, 1548–155.
- (22) Pankove, J. I. *Optical Process in Semiconductors*; Dover: New York, 1975.
- (23) Sutter, E.; Sutter, P.; Calarco, R.; Stoica, T.; Meijers, R. *Appl. Phys. Lett.* **2007**, *90*, 093118.
- (24) Popescu, C.; Stoica, T. *Phys. Rev. B* **1992**, *46*, 15063.
- (25) Franz, W. *Z. Naturforsch.* **1958**, *13*, 484.
- (26) Keldysh, L. V. *Sov. Phys. JETP* **1958**, *7*, 788.
- (27) Duke, C. B.; Alferieff, M. E. *Phys. Rev. B* **1966**, *145*, 2.
- (28) Dow, J. D.; Redfield, D. *Phys. Rev. B* **1970**, *1*, 3358.
- (29) Haug, H.; Koch, S. W. *Quantum Theory of the Optical and Electronic Properties of Semiconductors*; World Scientific Publishing: River Edge, NJ, 1994; p 343.
- (30) Peng, H. Y.; McCluskey, M. D.; Gupta, Y. M.; Kneissl, M.; Johnson, N. M. *Appl. Phys. Lett.* **1989**, *82*, 2085.
- (31) Pankove, J. I.; Moustakas, T. D. *Semiconductors and Semimetals-Gallium Nitride (GaN) I*; Academic Press: New York, 1998; p 313.
- (32) Segev, D.; Van de Walle, C. G. *Europhys. Lett.* **2006**, *76*, 305.
- (33) Kočan, M.; Rizzi, A.; Lüth, H.; Keller, S.; Mishra, U. K. *Phys. Status Solidi B* **2002**, *234*, 773.
- (34) Van de Walle, C. G.; Segev, D. *J. Appl. Phys.* **2007**, *101*, 081704.

NL0709540